LA-3810

C.3

LOS ALAMOS SCIENTIFIC LABORATORY
of the
University of California
LOS ALAMOS • NEW MEXICO

The Effect of Basic Neutron Reaction Cross Sections of Nitrogen (n,n′), (n,2n), (n,γ), (n,p) and (n,α) on High Energy Neutron Penetration in Air

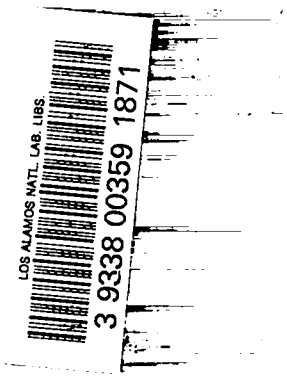

UNITED STATES
ATOMIC ENERGY COMMISSION
CONTRACT W-7405-ENG. 36

This report expresses the opinions of the author or authors and does not necessarily reflect the opinions or views of the Los Alamos Scientific Laboratory.

Printed in the United States of America. Available from Clearinghouse for Federal Scientific and Technical Information National Bureau of Standards, U. S. Department of Commerce Springfield, Virginia 22151

Price: Printed Copy $3.00; Microfiche $0.65

LA-3810
UC-34, PHYSICS
TID-4500

LOS ALAMOS SCIENTIFIC LABORATORY
of the
University of California
LOS ALAMOS • NEW MEXICO

Report written: October 1, 1967
Report distributed: December 7, 1967

The Effect of Basic Neutron Reaction Cross Sections of Nitrogen (n,n′), (n,2n), (n,γ), (n,p) and (n,α) on High Energy Neutron Penetration in Air

by

G. E. Hansen and H. A. Sandmeier

THE EFFECT OF BASIC NEUTRON REACTION CROSS SECTIONS OF NITROGEN (n,n'), (n,2n), (n,γ), (n,p) AND (n,α) ON HIGH ENERGY NEUTRON PENETRATION IN AIR

by

G. E. Hansen and H. A. Sandmeier

ABSTRACT

In an evaluation of an integral quantity one is interested in the relative sensitivity of this quantity to the basic input data.

This report assesses numerically the influence of the basic reaction cross section of nitrogen, the major constituent of air, on the penetration of high energy neutrons in air. The reaction cross sections investigated are (n,n'), (n,2n), (n,γ), (n,p) and (n,α). The collision cross section is kept constant in all perturbations and the above individual reaction cross sections are assumed to become elastic scattering collisions, i.e., (n,n') $\rightarrow$ (n,n) $\cdots\cdots$ (n,p) $\rightarrow$ (n,n). For a 10 m spherical source of (12-14) Mev neutron we evaluate unperturbed and perturbed neutron fluxes as a function of energy and distance. Numerical values for both flux and energy spectra are given at a distance of 825 m. As a representative example of integral data we evaluate the first collision dose to soft tissue for the perturbed and unperturbed neutron flux. It is concluded that the (n,n') $\rightarrow$ (n,n) and the (n,p) $\rightarrow$ (n,n) perturbations result in an increase of the dose by a factor of 2 whereas the (n,α) $\rightarrow$ (n,n) perturbation increases the dose by a factor of 1.8. The effect of the (n,2n) and (n,γ) perturbation causes insignificant perturbations in the first collision dose. One of us (H.A.S.) in a classified report has also investigated the influence of the above perturbations in the basic nitrogen cross section data to the neutron vulnerability of nuclear weapons.

The present report follows a previous publication including the same authors where the effect of calculational methods of the deep penetration of high energy neutron in air has been investigated.

Introduction. The numerical evaluation of the neutron flux in air due to a high energy neutron source depends mainly on

a. Method of calculation.

b. Basic cross sections used.

In previous publications (Ref. 1 and 2) we have investigated in detail the methods of calculations by means of multitable S_n-transport calculations which represent the scattering anisotropies at high energies with variable degree of accuracy.

This report assesses the influence of the basic reaction cross section of nitrogen, the major constituent of air (~80%), on the numerical values of the high energy neutron flux at 825 m distance. The reactions investigated are (n,n'), (n,2n), (n,γ), (n,p) and (n,α). The collision cross section is kept constant in all perturbations, namely (n,n') → (n,n), (n,2n) → (n,n) ····· (n,α) → (n,n).

The justification for the chosen perturbation is the fact that the collision cross section being determined by a transmission experiment can usually be evaluated quite accurately. Most uncertainties exist between the split up of nonelastic and elastic scattering reactions. The same philosophy applies to the perturbation in the absorption cross sections where the collision cross section is again held constant and individual absorptions (n,γ), (n,p) and (n,α) are assumed to become elastic scattering events.

The resulting changes in the flux vary in magnitude depending on the reactions which are perturbed. Since the (n,2n) cross section is very small in magnitude, it will cause a small perturbation in the flux and we can therefore evaluate the sensitivity of the (n,2n) reaction theoretically by means of first-order perturbation theory (Ref. 3). In this report we are not concerned with the theoretical correlation and simply substitute a perturbed cross section set and evaluate the resulting flux with the DTF-IV IASL S_n-transport code. For this study we have used the 1-table-weapons-transport approximation described in Ref. 1, p. 53.

This recipe differs from the regular 1-table-transport approximation reported also in Ref. 1, p. 49, only by the fact that the 1-table-weapons-transport uses flux averaging schemes only, whereas the regular 1-table-transport approximation uses flux-and-current averaging schemes for the cross sections generated from the LRL-IASL tape. No undue importance should be given to this fact here and the results using either set would lead to the same conclusion with which this investigation is concerned.

After the unperturbed and perturbed neutron spectra is obtained at 825 m distance due to a monoenergetic source of (12-14) Mev neutrons, one would like to associate a physical effect with the total neutron flux $\sum_g \phi_{i,g}$. Here we have chosen to evaluate the first collision dose to soft tissue as presented in (Ref. 4).

The "target" in this case, the first collision dose in ergs/gram received by man, is "selective" in classifying neutron energy groups in importance. The conclusions reached with respect to first collision dose can be completely different for another target which "classifies" neutron energy groups according to another set of "importance" numbers. The report by one of us (H.A.S.) in the classified literature (Ref. 5) is the subject of such an investigation.

I. Microscopic Cross Sections of N and O.

The cross sections, and associated nuclear data, used in these calculations are those of the LRL-IASL neutron data tape library as of October 1966. The numerical values for nitrogen and oxygen differ slightly from the values reported in Ref. 1.

The recipe used to generate the S_n-input cross sections for the 1-table weapons transport approximation is discussed in Ref. 1 and is repeated here in Table 1.

$$\Sigma_g = \Sigma_g(o) - \Sigma_{1,g}(o)$$

$$\Sigma^{(1)}_{g'\to g} = \Sigma_{o,g'\to g}(o) - \Sigma_{1,g'\to g}(o) \qquad (g' \neq g)$$

$$\Sigma^{(1)}_{g\to g} = \Sigma_{o,g\to g}(o) - \Sigma_{1,g\to g}(o)$$

$$\Sigma_a = \Sigma_g - \left[\sum_{g'\neq g} \Sigma^{(1)}_{g\to g'} + \Sigma^{(1)}_{g\to g}\right]$$

Table 1. S_n-input for 1-table-weapons-transport approximation (p. 53, IA-3415).

The energy group structure is also the same as in Ref. 1 and is repeated here in Table 2.

Group g	Energy E	$\Delta E = E_n - E_{n+1}$	E_n/E_{n+1}	$u = \ell n\, E_o/E_n$ (E_o = 14 MeV)	$\Delta u = \ell n \frac{E_n}{E_{n+1}}$	$1/\Delta u$	$\bar{v}\left[\frac{cm}{sec}\right] \times 10^{-8}$
1	12-14 MeV	2 MeV	1.1666	.1536	.1536	6.5104	50
2	8.3-12 MeV	3.7 MeV	1.4458	.5222	.3686	2.7130	43
3	5.3-8.3 MeV	3 MeV	1.5660	.9707	.4485	2.2297	36
4	3.4-5.3 MeV	1.9 MeV	1.5588	1.4146	.4439	2.2528	29
5	2.2-3.4 MeV	1.2 MeV	1.5455	1.8499	.4353	2.2973	23
6	1.4-2.2 MeV	.8 MeV	1.5714	2.2999	.4520	2.2124	19.0
7	0.9-1.4 MeV	.5 MeV	1.5556	2.7416	.4417	2.2640	15.0
8	0.58-0.9 MeV	.32 MeV	1.5517	3.1809	.4393	2.2763	12.0
9	370-580 KeV	210 KeV	1.5676	3.6304	.4495	2.2247	9.5
10	240-370 KeV	130 KeV	1.5417	4.0633	.4329	2.3100	7.6
11	150-240 KeV	90 KeV	1.6000	4.5333	.4700	2.1277	7.2
12	100-150 KeV	50 KeV	1.5	4.8387	.4054	2.4667	4.9
13	31.6-100 KeV	69 KeV	3.2258	6.1098	1.1711	.8539	3.28
14	10-31.6 KeV	21 KeV	3.1	7.2412	1.1314	.8839	1.78
15	3.16-10 KeV	6.84 KeV	3.1646	8.3932	1.1520	.8681	1.02
16	1-3.16 KeV	2.16 KeV	3.16	9.5437	1.1505	.8692	.57
17	.316-1 KeV	.684 KeV	3.1646	10.696	1.1520	.8681	.32
18	100-316. eV	216 eV	3.16	11.846	1.1505	.8692	.16
19	31.6-100 eV	68.4 eV	3.1646	12.998	1.1520	.8681	.10
20	10-31.6 eV	21.6 eV	3.16	14.149	1.1505	.8692	.057
21	3.16-10 eV	6.84 eV	3.1646	15.301	1.1520	.8681	.032
22	1-3.16 eV	2.16 eV	3.16	16.451	1.1505	.8692	.018
23	.316-1 eV	.684 eV	3.1646	17.603	1.1520	.8681	.010
24	.026-.316 eV	.290 eV	12.1538	20.101	2.4976	.4004	.004
25	Thermal .025-.026 eV	.001 eV	1.04	20.14	.0392	25.57	.002

Table 2. 25 energy group structure (IA-3415, p. 54).

I-1. Nitrogen Unperturbed.

The unperturbed S_n-input is shown in Table 3. In order to generate the "perturbed" S_n-input for nitrogen we need the "unperturbed" S_n-input for all individual reactions, namely (n,n); (n,n'); (n,2n); (n,γ); (n,p) and (n,α). Tables 4, 5, 6, and 7.

Table 3.

Microscopic cross sections of nitrogen for unperturbed 1-tbl-tr

(IRL-IASL data Oct. '66) neutron flux in air.

g	σ_a	σ_{tr}	$\sigma_{g\to g}$	$\sigma_{g\to g+1}$	$\sigma_{g\to g+2}$	$\sigma_{g\to g+3}$	$\sigma_{g\to g+4}$	$\sigma_{g\to g+5}$	$\sigma_{g\to g+6}$	$\sigma_{g\to g+7}$	$\sigma_{g\to g+8}$
1	7.05 -2	1.04 +0	7.73 -2	3.08 -1	1.04 -1	1.36 -1	1.03 -1	1.29 -1	6.40 -2	2.68 -2	1.13 -2
2	1.04 -1	9.64 -1	3.39 -1	2.09 -1	5.19 -2	8.83 -2	8.29 -2	5.30 -2	2.33 -2	8.05 -3	2.81 -3
3	1.76 -1	1.11 +0	4.33 -1	4.40 -1	1.98 -2	1.39 -2	1.64 -2	8.17 -3	2.70 -3	1.68 -4	0.0
4	3.54 -1	1.43 +0	6.23 -1	4.48 -1	3.60 -3	1.94 -3	2.38 -4	0.0	0.0	0.0	
5	2.07 -1	1.40 +0	7.26 -1	4.63 -1	0.0	2.91 -4	0.0				
6	9.07 -2	1.72 +0	1.08 +0	5.49 -1		0.0					
7	4.15 -2	1.60 +0	1.19 +0	3.68 -1							
8	4.57 -2	1.76 +0	1.22 +0	4.95 -1	0	0	0	0	0	0	0
9	1.95 -2	2.30 +0	1.51 +0	7.73 -1							
10	1.77 -3	2.77 +0	1.91 +0	8.52 -1							
11	1.50 -3	3.22 +0	2.32 +0	8.99 -1							
12	1.50 -3	3.73 +0	2.49 +0	1.23 +0							
13	1.61 -3	4.71 +0	4.07 +0	6.37 -1							
14	2.22 -3	5.45 +0	4.72 +0	7.27 -1							
15	4.03 -3	6.11 +0	5.30 +0	8.12 -1							
16	7.17 -3	7.10 +0	6.13 +0	9.57 -1							
17	1.27 -2	8.20 +0	7.11 +0	1.08 +0							
18	2.22 -2	8.98 +0	7.81 +0	1.15 +0							
19	4.03 -2	9.38 +0	8.15 +0	1.19 +0							
20	7.17 -2	9.57 +0	8.30 +0	1.20 +0							
21	1.27 -1	9.76 +0	8.41 +0	1.22 +0							
22	2.26 -1	9.96 +0	8.51 +0	1.22 +0							
23	4.02 -1	1.01 +1	8.47 +0	1.22 +0							
24	8.62 -1	1.07 +1	9.67 +0	1.74 -1							
25	1.85 +0	1.23 +1	1.04 +1								

g	$\sigma_{g\to g+9}$	$\sigma_{g\to g+10}$	$\sigma_{g\to g+11}$	$\sigma_{g\to g+12}$	$\sigma_{g\to g+13}$	$\sigma_{g\to g+14}$
1	5.15 -3	4.54 -3	1.17 -3	5.12 -4	4.86 -5	5.03 -6
2	1.25 -3	4.43 -4	3.20 -4	3.04 -5	3.15 -6	0
3	0	0	0	0	0	
4						
5						
.						
.						
.						
.						
.						
.						
25	0	0	0	0	0	0

Table 4.

Microscopic (n,n) cross sections of nitrogen for unperturbed 1-tbl-tr

(LRL-IASL data Oct. '66) neutron flux in air.

	$\Phi_o;P_o$			$\Phi_o;P_1$		
g	$\sigma^{n,n}_{o,g}(o)$	$\sigma^{n,n}_{o,g\to g}(o)$	$\sigma^{n,n}_{o,g\to g+1}(o)$	$\sigma^{n,n}_{1,g}(o)$	$\sigma^{n,n}_{1,g\to g}(o)$	$\sigma^{n,n}_{1,g\to g+1}(o)$
1	8.95 -1	5.87 -1	3.08 -1	5.10 -1	5.06 1	4.11 -3
2	9.83 -1	7.81 -1	2.02 -1	4.43 -1	4.83 -1	-4.02 -2
3	1.16 +0	7.39 -1	4.18 -1	3.06 -1	4.10 -1	-1.04 -1
4	1.34 +0	8.90 -1	4.47 -1	2.66 -1	4.85 -1	-2.19 -1
5	1.32 +0	8.59 -1	4.63 -1	1.33 -1	2.60 -1	-1.27 -1
6	1.84 +0	1.29 +0	5.49 -1	2.13 -1	3.60 -1	-1.47 -1
7	1.89 +0	1.52 +0	3.68 -1	3.33 -1	4.44 -1	-1.11 -1
8	1.87 +0	1.37 +0	4.95 -1	1.55 -1	3.27 -1	-1.72 -1
9	2.40 +0	1.63 +0	7.73 -1	1.19 -1	3.79 -1	-2.59 -1
10	2.91 +0	2.05 +0	8.52 -1	1.40 -1	4.05 -1	-2.65 -1
11	3.39 +0	2.49 +0	8.99 -1	1.63 -1	4.42 -1	-2.80 -1
12	3.91 +0	2.68 +0	1.23 +0	1.88 -1	5.71 -1	-3.83 -1
13	4.95 +0	4.31 +0	6.37 -1	2.38 -1	4.25 -1	-1.88 -1
14	5.72 +0	5.00 +0	7.27 -1	2.75 -1	4.90 -1	-2.15 -1
15	6.42 +0	5.60 +0	8.12 -1	3.08 -1	5.48 -1	-2.40 -1
16	7.45 +0	6.49 +0	9.57 -1	3.58 -1	6.40 -1	-2.82 -1
17	8.60 +0	7.52 +0	1.08 +0	4.13 -1	7.33 -1	-3.20 -1
18	9.41 +0	8.26 +0	1.15 +0	4.52 -1	7.94 -1	-3.42 -1
19	9.81 +0	8.62 +0	1.19 +0	4.71 -1	8.23 -1	-3.53 -1
20	9.98 +0	8.78 +0	1.20 +0	4.79 -1	8.36 -1	-3.56 -1
21	1.01 +1	8.90 +0	1.22 +0	4.86 -1	8.49 -1	-3.63 -1
22	1.02 +1	9.00 +0	1.22 +0	4.91 -1	8.55 -1	-3.64 -1
23	1.02 +1	8.96 +0	1.22 +0	4.89 -1	8.51 -1	-3.62 -1
24	1.03 +1	1.02 +1	1.74 -1	4.97 -1	5.48 -1	-5.12 -2
25	1.09 +1	1.09 +1		5.25 -1	5.25 -1	

Table 5.

Microscopic (n,n′) cross sections of nitrogen for unperturbed 1-tbl-tr

(LRL-LASL data Oct. '66) neutron flux in air.

g	$\sigma^{n,n'}_{o,g}(o)$	$\sigma^{n,n'}_{o,g\to g}(o)$	$\sigma^{n,n'}_{o,g\to g+1}(o)$	$\sigma^{n,n'}_{o,g\to g+2}(o)$	$\sigma^{n,n'}_{o,g\to g+3}(o)$	$\sigma^{n,n'}_{o,g\to g+4}(o)$	$\sigma^{n,n'}_{o,g\to g+5}(o)$	$\sigma^{n,n'}_{o,g\to g+6}(o)$
1	5.82 -1	0.0	0.0	1.04 -1	1.36 -1	1.03 -1	1.29 -1	6.40 -2
2	3.19 -1	0.0	6.98 -3	5.19 -2	8.83 -2	8.29 -2	5.30 -2	2.33 -2
3	8.44 -2	6.98 -4	2.25 -2	1.98 -2	1.39 -2	1.64 -2	8.17 -3	2.70 -3
4	6.80 -3	0.0	1.03 -3	3.60 -3	1.94 -3	2.38 -4	0.0	0.0
5	2.91 -4	0.0	0.0	0.0	2.91 -4	0.0	0.0	0.0
.	↓	↓	↓	↓	↓	↓	↓	↓
.	↓	↓	↓	↓	↓	↓	↓	↓
.	↓	↓	↓	↓	↓	↓	↓	↓
25	0	0	0	0	0	0	0	0

g	$\sigma^{n,n'}_{o,g\to g+7}(o)$	$\sigma^{n,n'}_{o,g\to g+8}(o)$	$\sigma^{n,n'}_{o,g\to g+9}(o)$	$\sigma^{n,n'}_{o,g\to g+10}(o)$	$\sigma^{n,n'}_{o,g\to g+11}(o)$	$\sigma^{n,n'}_{o,g\to g+12}(o)$	$\sigma^{n,n'}_{o,g\to g+13}(o)$	$\sigma^{n,n'}_{o,g\to g+14}(o)$
1	2.68 -2	1.13 -2	4.49 -3	1.99 -3	7.08 -4	5.12 -4	4.86 -5	5.03 -6
2	8.05 -3	2.81 -3	1.25 -3	4.43 -4	3.20 -4	3.04 -5	3.15 -6	
3	1.68 -4	0.0	0.0	0.0	0.0	0.0	0.0	0.0
.	↓	↓	↓	↓	↓	↓	↓	↓
.	↓	↓	↓	↓	↓	↓	↓	↓
.	↓	↓	↓	↓	↓	↓	↓	↓
25	0	0	0	0	0	0	0	0

Table 6.

Microscopic (n,2n) cross sections of nitrogen for unperturbed 1-tbl-tr (LRL-IASL data Oct. '66) neutron flux in air.

g	$\sigma^{n,2n}_{o,g}(o)$	$\sigma^{n,2n}_{o,g\to g}(o)$	$\sigma^{n,2n}_{o,g\to g+1}(o)$	$\sigma^{n,2n}_{o,g\to g+2}(o)$	$\sigma^{n,2n}_{o,g\to g+3}(o)$	$\sigma^{n,2n}_{o,g\to g+4}(o)$	$\sigma^{n,2n}_{o,g\to g+5}(o)$
1	1.83 -3	0.0	0.0	0.0	0.0	0.0	0.0
2	0.0	0.0	0.0	0.0	0.0	0.0	0.0
.	↓	↓	↓	↓	↓	↓	↓
.							
.							
25	0	0	0	0	0	0	0

g	$\sigma^{n,2n}_{o,g\to g+6}(o)$	$\sigma^{n,2n}_{o,g\to g+7}(o)$	$\sigma^{n,2n}_{o,g\to g+8}(o)$	$\sigma^{n,2n}_{o,g\to g+9}(o)$	$\sigma^{n,2n}_{o,g\to g+10}(o)$	$\sigma^{n,2n}_{o,g\to g+11}(o)$
1	0.0	0.0	0.0	6.59 -4	2.55 -3	4.58 -4
2	0.0	0.0	0.0	0.0	0.0	0.0
.	↓	↓	↓	↓	↓	↓
.						
.						
25	0	0	0	0	0	0

Table 7.

Microscopic (n,γ); (n,p) and (n,α) cross sections of nitrogen for unperturbed 1-tbl-tr (IRL-IASL data Oct. '66) neutron flux in air.

g	$\sigma_{o,g}^{n,\gamma}(o)$	$\sigma_{o,g}^{n,p}(o)$	$\sigma_{o,g}^{n,\alpha}(o)$
1	0.0	1.66 -2	5.57 -2
2		1.95 -2	8.49 -2
3		2.34 -2	1.53 -1
4		4.89 -2	3.05 -1
5		4.76 -2	1.60 -1
6		4.04 -2	5.03 -2
7		3.39 -2	7.55 -3
8		4.57 -2	0.0
9		1.95 -2	
10		1.77 -3	
11		1.50 -3	
12		1.50 -3	
13		1.61 -3	
14		2.22 -3	
15		4.03 -3	
16		7.17 -3	
17	0	1.27 -2	
18	2.44 -5	2.22 -2	
19	1.60 -3	3.87 -2	
20	3.35 -3	6.84 -2	
21	6.17 -3	1.21 -1	
22	1.13 -2	2.15 -1	
23	2.03 -2	3.82 -1	
24	3.85 -2	8.23 -1	
25	7.46 -2	1.77 +0	0

I-2. Nitrogen Perturbed.

As mentioned previously, we want to keep the collision cross section constant in all perturbations. Also the individual reactions (n,n'), (n,2n), (n,γ), (n,p) and (n,α) are assumed to become elastic scattering events; i.e., (n,n). Let us consider the perturbation in (n,n') to show how the perturbed cross section sets have been generated.

The unperturbed S_n-input on the LHS of the Boltzmann equation is σ_g, the collision cross section, and on the RHS of the B.E. we have $\sigma^{(1)}_{g\to g}$ and several $\sigma^{(1)}_{g'\to g}$. Let us now generate a perturbed set of S_n-input cross sections where the inelastic scattering (n,n') has been set to zero and denote these with '. We get a new set, namely σ'_g, $\sigma^{(1)'}_{g\to g}$ and several $\sigma^{(1)'}_{g'\to g}$. Symbolically we have

$$\text{unperturbed set} \quad \sigma_g,\ldots\ldots\sigma^{(1)}_{g\to g},\sigma^{(1)}_{g'\to g}\ldots\ldots \tag{1}$$

$$\text{perturbed set } (\sigma^{n,n'}=0) \quad \sigma'_g,\ldots\ldots\sigma^{(1)'}_{g\to g},\sigma^{(1)'}_{g'\to g}\ldots\ldots . \tag{2}$$

We now add to both sides of the B.E. (2)

$$\sigma_g-\sigma'_g\ldots\ldots\sigma_g-\sigma'_g\ldots\ldots . \tag{3}$$

We get

$$\sigma_g\ldots\ldots\sigma^{(1)'}_{g\to g} + [\sigma_g-\sigma'_g],\ \sigma^{(1)'}_{g'\to g}\ldots . \tag{4}$$

The new set (4) has the same collision cross section as the unperturbed set (1) and the difference of $\sigma_g-\sigma'_g$ has been added to the perturbed in group scattering cross section $\sigma^{(1)'}_{g\to g}$. We have therefore accomplished what we set out to do in a perturbation; namely, keeping the collision cross section constant and letting the inelastic scattering become an elastic in-group scattering.

This procedure has been repeated for all perturbations leading to five perturbed cross section sets for nitrogen, namely (n,n')→(n,n), (n,2n)→(n,n), (n,σ)→(n,n), (n,p)→(n,n) and (n,α)→(n,n). We do not present these perturbed sets, as they can be constructed from the unperturbed data in Tables 3 through 7.

I-3. Oxygen.

The oxygen cross section was kept constant in this calculation for all perturbations in the nitrogen data.

II. Macroscopic Cross Sections of N and O.

The macroscopic cross sections of nitrogen and oxygen were obtained from the microscopic data discussed in I and the sea level air compositions quoted in (Ref. 1) p. 41, namely

1.22 gram/liter		sea level air normal day 15°C
nitrogen	79%	$4.024 \times 10^{-5} \times 10^{24}$ nuclei/cc
oxygen	21%	$1.070 \times 10^{-5} \times 10^{24}$ nuclei/cc.

III. Fast Neutron Penetration in Sea Level Air.

Using the unperturbed and perturbed 1-table-transport[1] cross sections sets, we have evaluated the neutron flux in a homogeneous sea level air atmosphere due to a gp 1 source of (12-14) Mev neutrons (10 m sphere, 1 neutron). The outer radius of the spherical one-dimensional, S_8, calculation was at 1100 meters and the flux was evaluated at 102 space points.

The numerical values of the group fluxes at 825 meters are listed in Table 8. The change in flux $\delta\Phi/\Phi$ at 825 m for the (n,n')→(n,n) and (n,p)→(n,n) perturbation as opposed to the unperturbed flux Φ is shown in Figs. 1 and 2.

Table 9 lists the spectral components and Figs. 3 and 4 show the spectrum for the (n,n')→(n,n) and (n,p)→(n,n) perturbation at 825 m.

In order that the reader is not misled by the appearance of a large peak in the spectrum for gp 25 with a small lethargy increment Δu as given in Table 2, we have changed gps 24 and 25 as follows. The energy E and lethargy limits u for gp 24 are E(.316-.0413 ev), u(17.603-19.64), i.e., Δu = 2.01 and for gp 25, E(.0413-.0152 ev), u = (19.64-20.64), i.e., Δu = 1.0. The area under a lethargy interval is proportional to the number of neutrons in this energy interval. For a small interval Δu, $4\pi R_i^2\Phi_{ig}/\Delta u$ will be large, giving the physical impression of a large neutron population in this energy interval. By choosing longer lethargy intervals, we will avoid this unphysical appearance. For the values of $\Phi_{i,g}$ we have however used the values given by the group structure given in Table 2.

---

[1] For simplicity we call here and subsequently the 1-table weapon transport approximation in LA-3415 p. 53, 1-table transport approximation.

Table 8.

Neutron flux in sea level air at 825 m due to gp 1 (12-14 Mev) source (10 m sphere, 1 neut.)

1-tbl-tr, LRL-LASL data N,O; Oct. '66.

Φ_g (825 m)

g	unperturbed	perturbed				
		n,n'→n,n	n,2n→n,n	n,γ→n,n	n,p→n,n	n,α→n,n
1	1.46 -13	7.58 -13	1.46 -13	1.46 -13	1.51 -13	1.65 -13
2	2.70 -13	1.62 -12	2.70 -13	2.69 -13	2.88 -13	3.54 -13
3	2.40 -13	8.22 -13	2.40 -13	2.40 -13	2.62 -13	3.90 -13
4	2.60 -13	5.83 -13	2.61 -13	2.60 -13	2.97 -13	5.95 -13
5	5.30 -13	7.49 -13	5.31 -13	5.30 -13	6.38 -13	1.29 -12
6	6.16 -13	6.37 -13	6.17 -13	6.16 -13	7.60 -13	1.35 -12
7	8.57 -13	7.81 -13	8.59 -13	8.57 -13	1.08 -12	1.67 -12
8	1.09 -12	8.68 -13	1.09 -12	1.09 -12	1.45 -12	1.94 -12
9	6.10 -13	4.70 -13	6.11 -13	6.10 -13	8.17 -13	1.06 -12
10	7.33 -13	5.38 -13	7.34 -13	7.33 -13	9.74 -13	1.24 -12
11	7.97 -13	5.63 -13	7.98 -13	7.97 -13	1.05 -12	1.32 -12
12	6.26 -13	4.31 -13	6.26 -13	6.26 -13	8.23 -13	1.02 -12
13	1.34 -12	8.85 -13	1.34 -12	1.34 -12	1.75 -12	2.14 -12
14	1.24 -12	7.96 -13	1.24 -12	1.24 -12	1.61 -12	1.96 -12
15	1.15 -12	7.23 -13	1.15 -12	1.15 -12	1.50 -12	1.80 -12
16	1.01 -12	6.21 -13	1.00 -12	1.00 -12	1.31 -12	1.56 -12
17	9.04 -13	5.52 -13	9.03 -13	9.03 -13	1.19 -12	1.39 -12
18	8.48 -13	5.13 -13	8.48 -13	8.48 -13	1.14 -12	1.30 -12
19	8.11 -13	4.86 -13	8.10 -13	8.12 -13	1.12 -12	1.24 -12
20	7.69 -13	4.57 -13	7.69 -13	7.72 -13	1.11 -12	1.17 -12
21	6.96 -13	4.11 -13	6.95 -13	7.02 -13	1.10 -12	1.05 -12
22	5.99 -13	3.51 -13	5.98 -13	6.08 -13	1.09 -12	9.03 -13
23	4.65 -13	2.71 -13	4.64 -13	4.78 -13	1.09 -12	6.99 -13
24	5.91 -13	3.42 -13	5.90 -13	6.31 -13	6.47 -12	8.85 -13
25	6.09 -14	3.51 -14	6.08 -14	6.78 -14	1.64 -11	9.10 -14

Table 9.

Spectral component for neutron flux in sea level air at 825 m

due to gp 1 (12-14 Mev) source (10 m sphere, 1 neut.).

g	$4\pi R_i^2/\Delta u$ (R=825 m)	$4\pi R_i^2 \Phi_{i,g}/\Delta u_g$ R = 825 m					
		unperturbed	perturbed				
			n,n'→n,n	n,2n→n,n	n,γ→n,n	n,p→n,n	n,α→n,n
1	5.5681 +11	8.1294 -2	4.2206 -1	8.1294 -2	8.1294 -2	8.4078 -2	9.1874 -2
2	2.3204 +11	6.2651 -2	3.7590 -1	6.2748 -2	6.2419 -2	6.6824 -2	8.0054 -2
3	1.9071 +11	4.5770 -2	1.5676 -1	4.5770 -2	4.5770 -2	4.9966 -2	7.4377 -2
4	1.9268 +11	5.0097 -2	1.1233 -1	5.0289 -2	5.0097 -2	5.7226 -2	1.1464 -1
5	1.9649 +11	1.0414 -1	1.4717 -1	1.0434 -1	1.0414 -1	1.2536 -1	2.5347 -1
6	1.8923 +11	1.1657 -1	1.2054 -1	1.1675 -1	1.1657 -1	1.4381 -1	2.5546 -1
7	1.9364 +11	1.6595 -1	1.5123 -1	1.6614 -1	1.6595 -1	2.0913 -1	3.2338 -1
8	1.9469 +11	2.1221 -1	1.6899 -1	2.1221 -1	2.1221 -1	2.8230 -1	3.7770 -1
9	1.9628 +11	1.1607 -1	8.9432 -2	1.1626 -1	1.1607 -1	1.5546 -1	2.0170 -1
10	1.9757 +11	1.4482 -1	1.0629 -1	1.4502 -1	1.4482 -1	1.9243 -1	2.4499 -1
11	1.8198 +11	1.4504 -1	1.0245 -1	1.4522 -1	1.4504 -1	1.9108 -1	2.4021 -1
12	2.1098 +11	1.3207 -1	9.0932 -2	1.3207 -1	1.3207 -1	1.7364 -1	2.1520 -1
13	7.3034 +10	9.7866 -2	6.4635 -2	9.7866 -2	9.7866 -2	1.2781 -1	1.5629 -1
14	7.5596 +10	9.3739 -2	6.0174 -2	9.3739 -2	9.3739 -2	1.2171 -1	1.4817 -1
15	7.4245 +10	8.5382 -2	5.3679 -2	8.5382 -2	8.5382 -2	1.1137 -1	1.3364 -1
16	7.4342 +10	7.5085 -2	4.6166 -2	7.4342 -2	7.4342 -2	9.7388 -2	1.1597 -1
17	7.4245 +10	6.7117 -2	4.0983 -2	6.7043 -2	6.7043 -2	8.8352 -2	1.0320 -1
18	7.4342 +10	6.3042 -2	3.8137 -2	6.3042 -2	6.3042 -2	8.4750 -2	9.6645 -2
19	7.4245 +10	6.0213 -2	3.6083 -2	6.0138 -2	6.0287 -2	8.3154 -2	9.2064 -2
20	7.4342 +10	5.7169 -2	3.3974 -2	5.7169 -2	5.7392 -2	8.2520 -2	8.6980 -2
21	7.4245 +10	5.1675 -2	3.0515 -2	5.1600 -2	5.2120 -2	8.1670 -2	7.7957 -2
22	7.4342 +10	4.4531 -2	2.6094 -2	4.4457 -2	4.5200 -2	8.1033 -2	6.7131 -2
23	7.4245 +10	3.4524 -2	2.0120 -2	3.4450 -2	3.5489 -2	8.0927 -2	5.1897 -2
24	4.2551 +10	2.5147 -2	1.4552 -2	2.5105 -2	2.6850 -2	2.8679 -1	3.7658 -1
25	8.5530 +10	5.2089 -3	3.0021 -3	5.2003 -3	5.7989 -3	1.4027 0	7.7832 -3

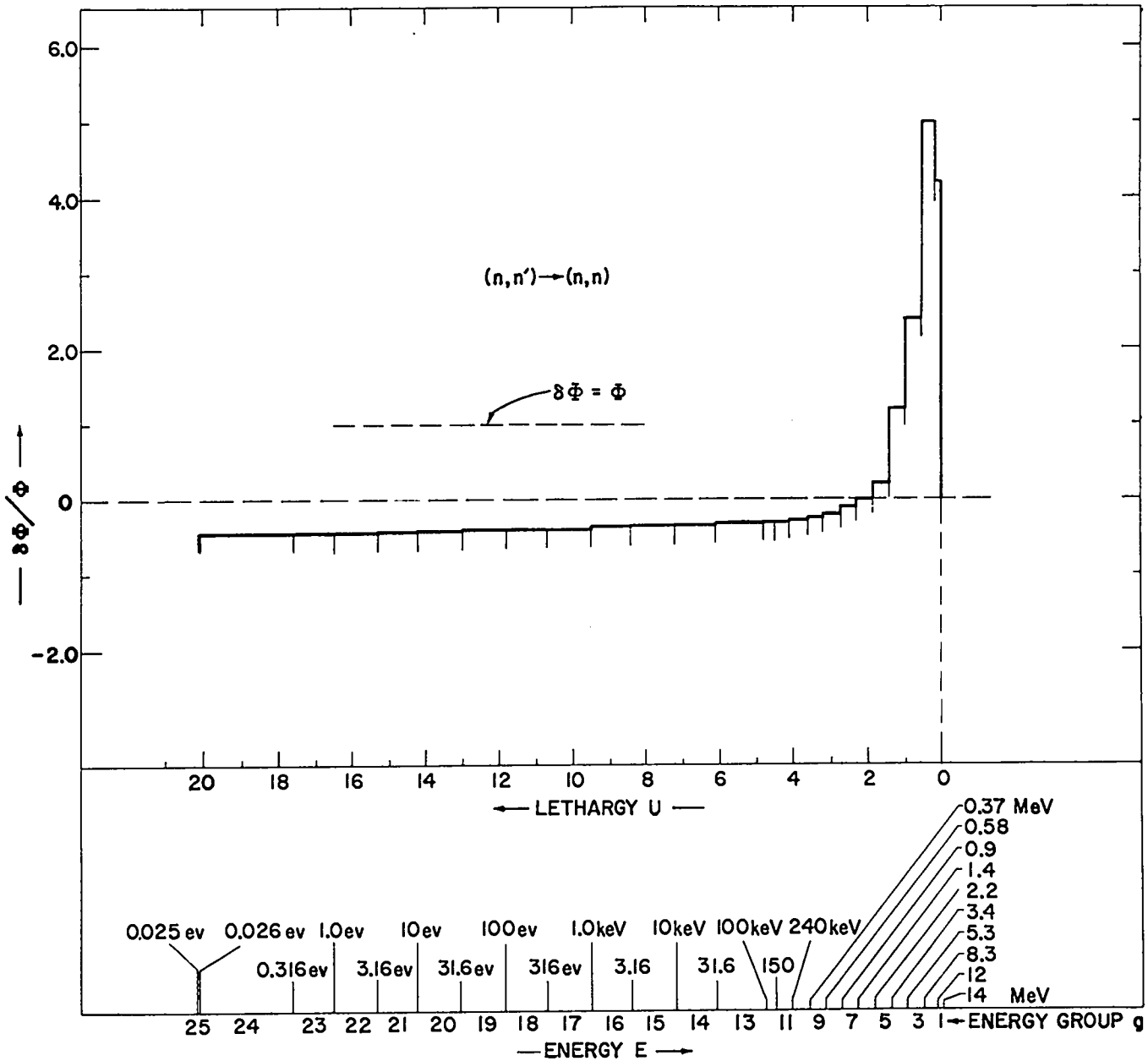

Fig. 1. Incremental flux $\delta\phi/\phi$ at 825 m for perturbation (n,n') → (n,n).

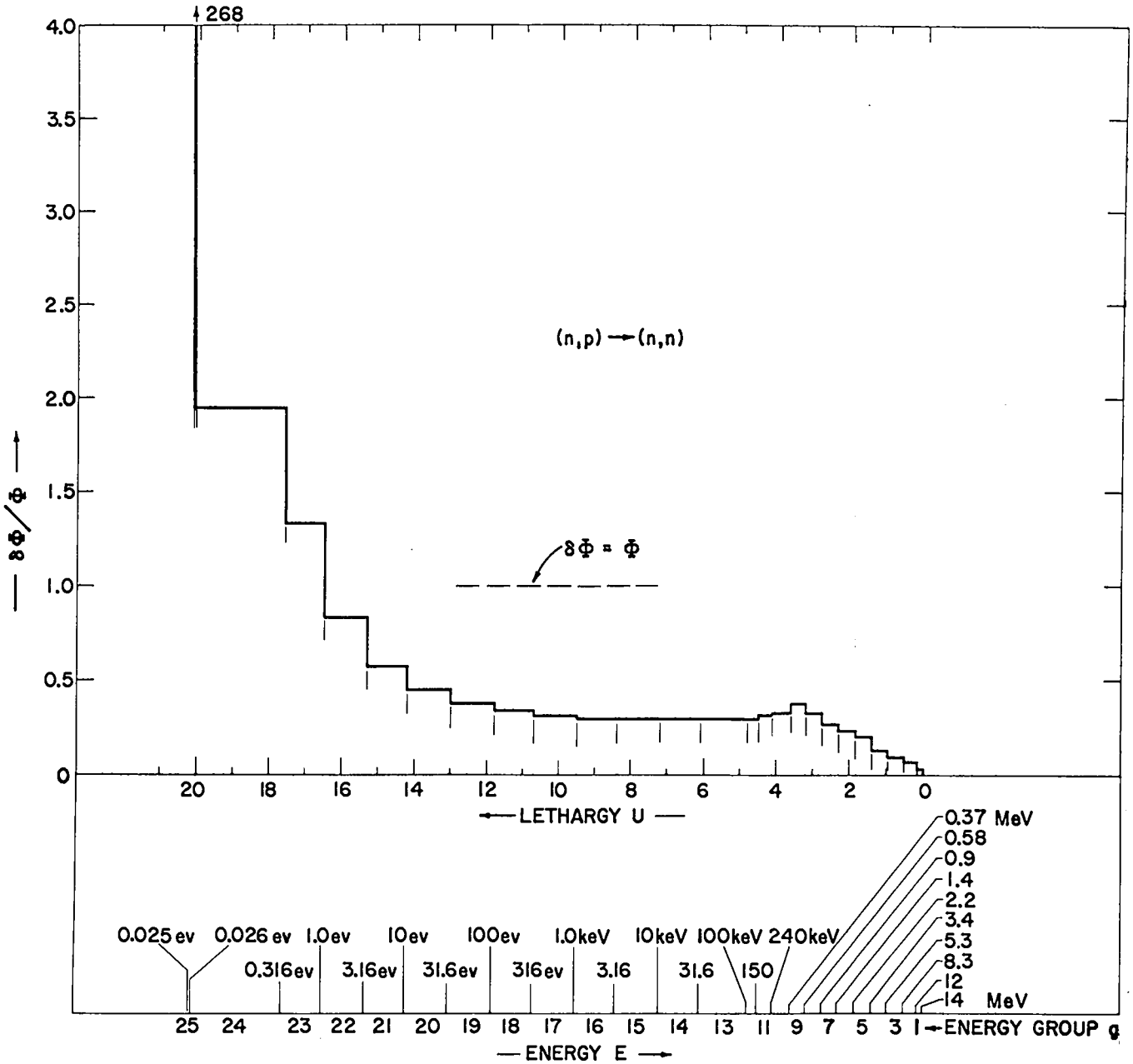

Fig. 2. Incremental flux $\delta\phi/\phi$ at 825 m for perturbation (n,p) → (n,n).

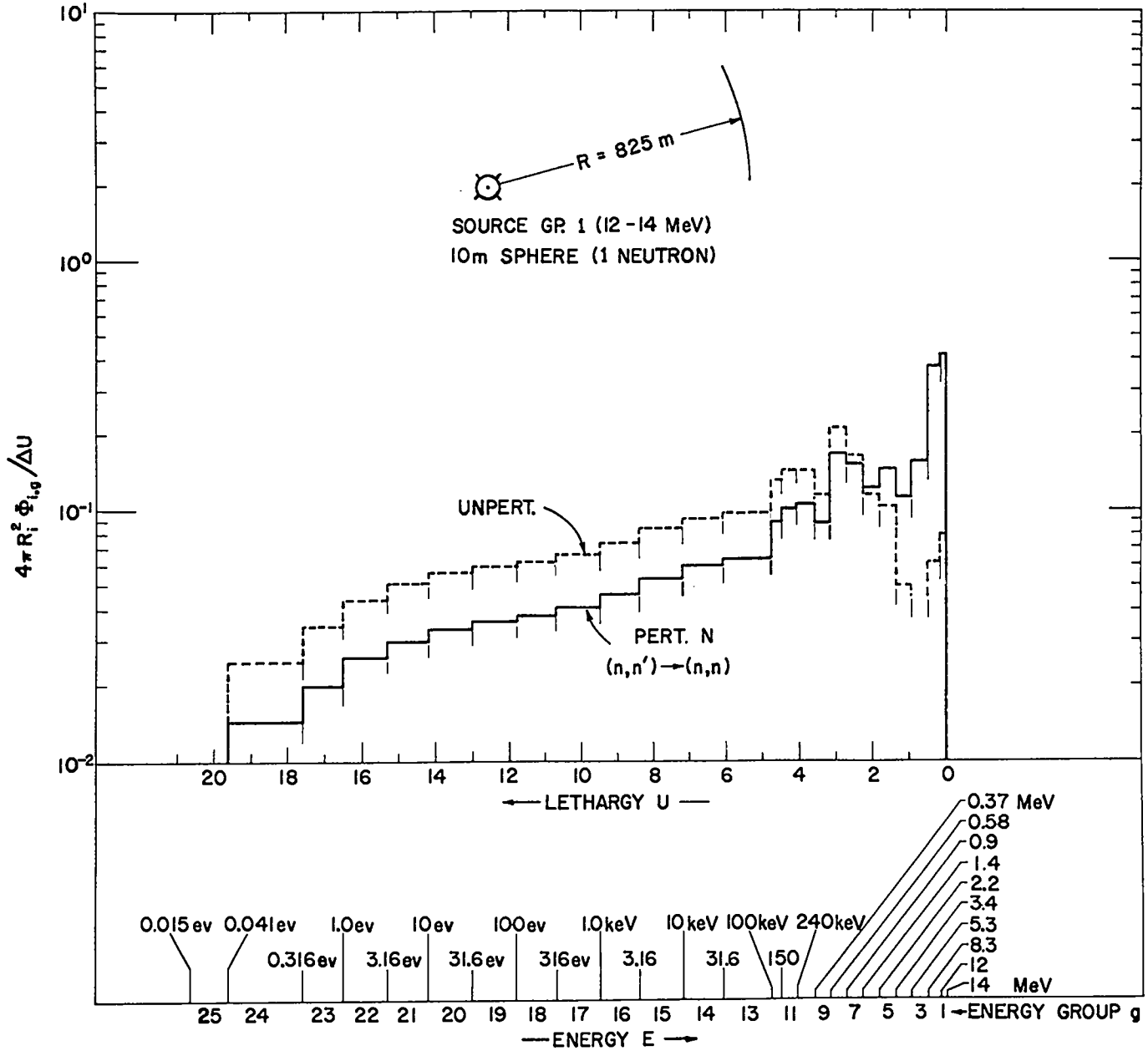

Fig. 3. Neutron spectrum in sea level air due to gp 1 (12-14 Mev) source (10 m sphere, 1 neut.) at 825 m distance. Unperturbed and perturbed N cross section. $\sigma(n,n') \rightarrow \sigma(n,n)$.

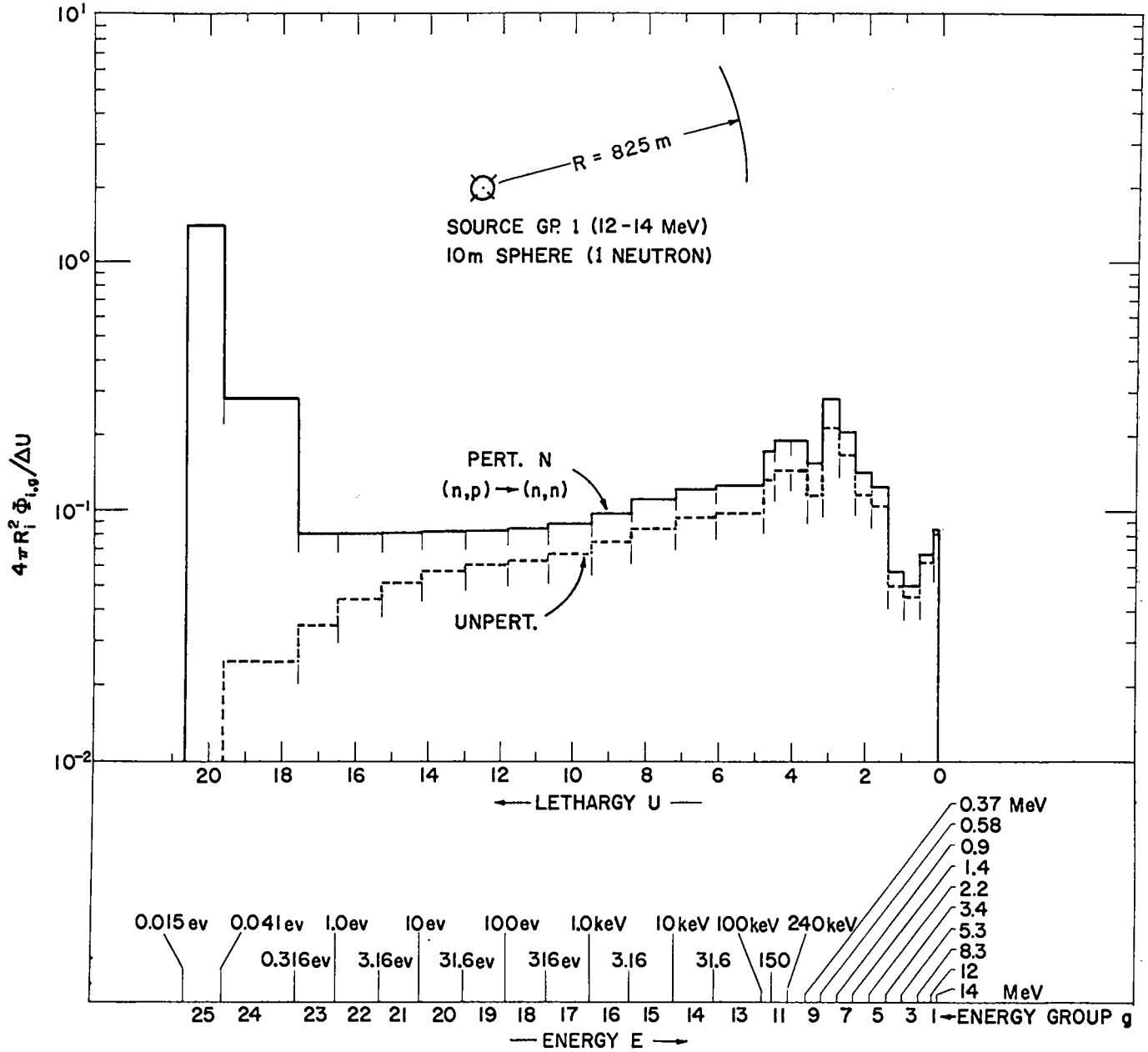

Fig. 4. Neutron spectrum in sea level air due to gp 1 (12-14 Mev) source (10 m sphere, 1 neut.) at 825 m distance. Unperturbed and perturbed N cross section $\sigma(n,p) \rightarrow \sigma(n,n)$.

IV. First Collision Dose.

The first collision dose numbers are taken from Ref. 5 and are listed in Table 10. The evaluated dose in ergs/gm x $4\pi R_i^2$ at 825 m sea level air is shown in Fig. 5.

ACKNOWLEDGMENTS

We would like to thank R. B. Lazarus for generating the perturbed cross section sets from the LRL-IASL tape. Dale Hankins helped us in the formulation of the first collision dose problem. The numerical evaluation of the first collision dose to man and related data was obtained with a "dose" code written by R. L. Berger of the University of California in Davis (Ref. 6). Dave Presbindowski from Purdue University has also assisted us in some of the tasks of this analysis.

REFERENCES

1. "Computation of Fast Neutron Penetration in Air by the 'S_n-Method' with Special Emphasis on the use of 'Multitable-Multigroup Cross Section Sets." Los Alamos Report 3415, Nov. 1965, H. A. Sandmeier, G. E. Hansen, R. L. Lazarus and R. J. Howerton (LRL).
2. "Multitable Treatments of Anisotropic Scattering in S_n Multigroup Transport Calculations." Nuclear Science and Engineering: 28, 367-383 (1967), G. I. Bell, G. E. Hansen, and H. A. Sandmeier.
3. "An Analysis of the Effects of Cross Section Uncertainties on the Multitable S_n Solution of Neutron Transport through Air." David Presbindowski, Ph.D. Thesis submitted to Department of Nuclear Engineering, Oct. 1967, Purdue University.
4. "Protection against Neutron Radiation up to 30 Million Electron Volts," Handbook 63, p. 7, U.S. Department of Commerce, National Bureau of Standards.
5. "The Effect of Basic Neutron Reaction Cross Section of Nitrogen in Air on Neutron Vulnerability Lethal Radii Calculations of Naval Nuclear Weapons." (Title unclassified.) U.S. Naval Weapon Evaluation Facility Report (to be published). J. L. Abbott, R. L. Berger, H. A. Sandmeier.
6. "Lethal Radii for Neutron Kill of Polaris MK 58, with Special Emphasis on Computerized Methods of Calculation." (Title unclassified.) U.S. Naval Weapons Evaluation Facility Report 1017, October 1967, R. L. Berger and H. A. Sandmeier (Consultant).

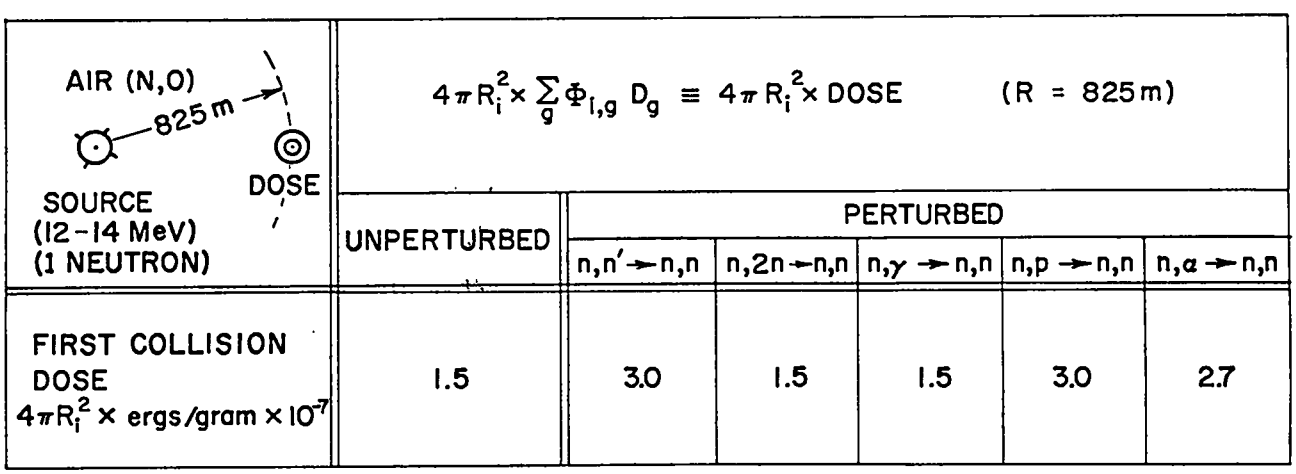

Fig. 5. First collision dose in man due to high energy neutron source at 825 m.

Table 10. First collision dose numbers.

Energy Group g	Energy E		First collision dose (ergs/g) per (neut/cm^2) x10^8
1	12-14	MeV	80.0
2	8.3-12	MeV	70.0
3	5.3-8.3	MeV	50.0
4	3.4-5.3	MeV	40.0
5	2.2-3.4	MeV	35.0
6	1.4-2.2	MeV	30.0
7	0.9-1.4	MeV	25.0
8	0.58-0.9	MeV	18.0
9	370-580	KeV	17.0
10	240-370	KeV	12.0
11	150-240	KeV	10.0
12	100-150	KeV	7.0
13	31.6-100	KeV	5.0
14	10-31.6	KeV	2.0
15	3.16-10	KeV	1.0
16	1-3.16	KeV	.20
17	.316-1	KeV	.12
18	100-316.	eV	.10
19	31.6-100	eV	.12
20	10-31.6	eV	.25
21	3.16-10	eV	.45
22	1-3.16	eV	.80
23	.316-1	eV	1.3
24	.026-.316		4.0
25	Thermal .025-.026	eV	7.0